Aigner, Philipp; Schlütter, Sebastian

Working Paper

Enhancing gradient capital allocation with orthogonal convexity scenarios

ICIR Working Paper Series, No. 47/23

Provided in Cooperation with:
International Center for Insurance Regulation (ICIR), Goethe University Frankfurt

Suggested Citation: Aigner, Philipp; Schlütter, Sebastian (2023) : Enhancing gradient capital allocation with orthogonal convexity scenarios, ICIR Working Paper Series, No. 47/23, Goethe University Frankfurt, International Center for Insurance Regulation (ICIR), Frankfurt a. M.

This Version is available at:
https://hdl.handle.net/10419/271086

Enhancing Gradient Capital Allocation with Orthogonal Convexity Scenarios *

Philipp Aigner† Sebastian Schlütter‡

Abstract

Gradient capital allocation, also known as Euler allocation, is a technique used to redistribute diversified capital requirements among different segments of a portfolio. The method is commonly employed to identify dominant risks, assessing the risk-adjusted profitability of segments, and installing limit systems. However, capital allocation can be misleading in all these applications because it only accounts for the current portfolio composition and ignores how diversification effects may change with a portfolio restructuring. This paper proposes enhancing the gradient capital allocation by adding "orthogonal convexity scenarios" (OCS). OCS identify risk concentrations that potentially drive portfolio risk and become relevant after restructuring. OCS have strong ties with principal component analysis (PCA), but they are a more general concept and compatible with common empirical patterns of risk drivers being fat-tailed and increasingly dependent in market downturns. We illustrate possible applications of OCS in terms of risk communication and risk limits.

JEL classification: G28, G32, D62, H23

Keywords: Risk capital allocation, Scenario analysis, Risk communication, Risk limiting, Principal Component Analysis

*We thank Kylie Braegelmann, Andrej Gill, Helmut Gründl, Markus Parlasca, Hato Schmeiser, and participants of the 2020 CEQURA conference, 2021 DVfVW annual meeting, 2021 IME congress, 2021 ARIA annual meeting and 2021 German Finance Association (DGF) annual meeting for their valuable comments.

†Mainz University of Applied Sciences, School of Business, Lucy-Hillebrand-Str. 2, 55128 Mainz, Germany; Johannes-Gutenberg University Mainz; email: philipp.aigner@hs-mainz.de

‡Mainz University of Applied Sciences, School of Business, Lucy-Hillebrand-Str. 2, 55128 Mainz, Germany; Fellow of the International Center for Insurance Regulation, Goethe University Frankfurt; email: sebastian.schluetter@hs-mainz.de

1 Introduction

Risk diversification within an investment portfolio or multi-segment firm can help to reduce the portfolio's potential loss. Capital needs for the portfolio, e.g. on the basis of Value-at-Risk or Expected Shortfall, are therefore typically lower for the portfolio than the sum of capital needs for the portfolio segments stand-alone. The gradient (synonymous Euler) capital allocation mechanism distributes the diversified risk measurement back to portfolio segments. It is thus a relatively simple tool to inform decision makers which segments are dominant risk drivers when accounting for risk diversification in the portfolio. Precisely speaking, the gradient capital allocation points out the marginal impact of segment volumes on diversified portfolio risk. It therefore allows for drawing conclusions about which segments to marginally expand or reduce to achieve an optimal risk-return profile (cf. Tasche, 2008).

The informative value of gradient capital allocation is limited, however, when realistically considering non-marginal portfolio changes. In fact, portfolio risk does not change linearly by a portfolio restructuring, as the structure of risk diversification changes. For example, risks of a fund's investments into a new asset category may be well diversified with other risks as long as the investments are of small volume. Yet, after expanding investments into the new category, these risks could substantially shape the bank's overall risk profile. Examples in Gründl and Schmeiser (2007, pp. 308-314) highlight errors in pricing of insurance contracts based on capital allocation when new contracts are added to an existing portfolio and hence the structure of the portfolio changes. Similarly, Buch et al. (2011) show that a control problem for portfolio optimization can fail when only relying on first-order derivatives; to reach the optimum, the authors propose a correction term that includes second-order derivatives. Likewise, Kang and Poshakwale (2019) make use of the the Hessian matrix of risk measurement to identify bank's optimal portfolio in a multi-period model. Gourieroux et al. (2000) identify an efficient stock portfolio—with risk being measured by Value-at-Risk instead of the variance—and to this end employ first and second-order derivatives of Value-at-Risk with respect to the asset allocation.

This paper suggests using the gradient capital allocation as a first scenario and incorporating a small set of additional "orthogonal convexity scenarios" (OCS). OCS capture second-order derivatives of the risk measurement, making them a valuable complement

to the gradient allocation. Notably, the primary purpose of OCS is not to circumvent recalculating the true risk of a new portfolio, but rather to communicate the portfolio's risk structure in simple terms, but more holistically than the gradient allocation does. Before explaining the applications of OCS in more detail, we describe the working of our approach, which can be divided into two steps.

Firstly, our approach builds on a second-order Taylor series of portfolio risk measurement which can be presented in terms of a well-known risk aggregation structure. To achieve this coincidence, our main assumption is that the portfolio risk measurement is a positive homogeneous and differentiable function in a *portfolio vector*, which contains the decision variables and characterizes the structure of the portfolio. Typically, but not necessarily, the elements of the portfolio vector are the volumes of the portfolio segments. Thanks to positive homogeneity, the second-order Taylor expansion of the risk measurement in square simplifies to a quadratic form in the portfolio vector (cf. Paulusch and Schlütter, 2022). The square-root of this quadratic form is structurally identical with the "hybrid approach" of risk measurement, which was proposed by Rosenberg and Schuermann (2006) and is used for example in the Solvency II standard formula of European insurance regulation. Therefore, when the hybrid approach is properly calibrated with a "sensitivity-implied tail correlation matrix", it locally approximates the original risk measurement including all first and second-order derivatives (Paulusch and Schlütter, 2022). This is true even if portfolio risk is subject to skewed and heavy-tailed distributions and increased tail dependencies.

Secondly, we tackle the issue that the information structure inherent in the calibration of the hybrid approach is still complex, especially in situations with many portfolio segments. To make it easier to understand for decision makers, we translate this information into deterministic scenarios which structurally resemble the gradient allocation. As explained in step one, we approximate portfolio risk with a quadratic form, which mimics the variance of a sum of random variables. For the latter, principal component analysis is a common tool to derive a linear decomposition into uncorrelated random variables. Our OCS generalize PCA: for portfolio risk following a multivariate elliptical distribution, OCS refer in fact to uncorrelated random variables. In general, OCS are orthogonal in the sense of marginal contributions of portfolio segments on diversified portfolio risk. Similar to PCA can be calculated based on the spectral decomposition of the covariance

matrix, the selection of OCS is possible based on an eigenvalue problem. We show that an OCS-based risk measurement reflects the original risk measurement in the sense of all first-order derivatives as well as second-order derivatives with regard to portfolio changes in a prespecified subspace.

We explain several applications of our proposed OCS approach to outline its advantages compared to traditional methods. In our example, the stochastic distributions of the segments' profits or losses used include skewed and heavy-tailed distributions which are partly connected with a Gumbel copula modeling increased tail dependencies. Portfolio risk is measured by the 99% Value-at-Risk of unexpected losses.

Our example substantiates that convexity of portfolio risk has to be evaluated from a holistic perspective. Considering a stylized financial institution with three business segments, the traditional gradient allocation (i.e. our first OCS) misses the true Value-at-Risk especially when the volumes of segments 1 and 2 move in the same direction (e.g. both are increased) but the volume of segment 3 moves in the opposite direction (is reduced). In terms of stochastic distributions, this is because segments 1 and 2 exhibit an increased tail dependence; segment 3 is well diversified in the initial portfolio, but it includes heavy-tailed risks that could become dominant if the segment is over-proportionally expanded. Accordingly, our second OCS assigns segments 1 and 2 values of the same sign, but segment 3 a value of the opposite sign. As for the gradient allocation, the values of all OCS can be regarded as a meaningful realization of the multivariate distribution of segment risks.

A first application of OCS is therefore to support the communication of risk concentrations and diversification effects between risk modelers on the one hand and decision makers and other stakeholders on the other. In fact, this communication has been regarded in the literature as both challenging and essential to establishing effective and value-adding Enterprise Risk Management.[1] While the gradient capital allocation is a relatively simple tool to communicate dominant risk drivers and natural hedging effects in the initial portfolio, our additional OCS point out what portfolio restructurings have a particiluarly large impact on risk diversification.

[1]Communication gaps between risk modelers and decision makers have been identified as a trigger of the 2007-2008 financial crisis, cf. (Stulz, 2008, p. 45) and Eling and Schmeiser (2010, p. 16), and are still considered as a central challenge in Enterprise Risk Management, cf. Wilson (2015, p. 599), Aven (2016, p. 10).

Secondly, OCS can support the graphical visualization of portfolio risk in order to provide another tool for risk communication or to serve as a starting point for validating the risk model. In a plot of multivariate realizations of the segment's profits or losses, OCS generally lie on the surface of an ellipsoid. The orientation of this ellipsoid reflects risk contributions in the initial portfolio (i.e. the gradient allocation), and its width reflects convexity of portfolio risk. In the special case of a multivariate elliptical distribution, the orientation of the ellipsoid coincides with the OLS regression function when regressing a segment's profits on the entire portfolio's profits; convexity of portfolio risk depends on the standard deviation of the regression's residuals.

Thirdly, the gradient capital allocation can be applied as a basis for breaking down a portfolio risk limit to portfolio segments.[2] In this sense, segments receiving higher amounts from the gradient allocation have a higher impact on the overall portfolio risk and should therefore be more strictly limited and monitored. However, the effectiveness of the limit system in this set-up is only ensured as long as the gradient allocation correctly reflects the risk structure of the portfolio, i.e. the composition of the portfolio may not change too much. OCS can help integrate the latter condition directly into the risk limit system. For this purpose, we propose risk limits of first and second order: while first-order limits are defined with the condition of the portfolio's risk structure remaining within certain constraints, second-order limits monitor whether this condition is met. We demonstrate that second-order limits are tight for segments that exert a strong convex impact on diversified capital and are hence likely to become relevant risk drivers; segments with a slight convex impact, in turn, receive a loose limit.

Our paper contributes to the literature in several ways. From a management science perspective, the gradient captial allocation can be seen as a differentiation-based method of sensitivity analysis,[3] serving as a crucial link between risk modeling and decision-making. While the classical gradient capital allocation offers a first-order Taylor expansion, OCS provide additional insights in terms of second-order sensitivities. Our basic assumption, positive homogeneity, is satisfied by common risk measures, such as Value-at-Risk and Expected Shortfall[4]; other examplies of positive homogeneous risk measures can be found

[2] Cf. Jorion (2006), Buch et al. (2011), Erel et al. (2015).

[3] For an overview on this method, cf. Borgonovo and Plischke (2016, p. 873 f.).

[4] Sensitivities of Value-at-Risk are studied by Gourieroux et al. (2000), those of Expected Shortfall are studied by Hong and Liu (2009).

in Landsman and Makov (2011) and McNeil et al. (2015, p. 77). Moreover, an example for a positive homogeneous risk measure is presented by Bauer and Zanjani (2016) through determining economically correct marginal capital costs in a first step and then deriving a risk measure with appropriate sensitivities in a second step. Since our scenarios are deterministic vectors, our approach differs from Schilling et al. (2020), who decompose the portfolio loss into additive stochastic components; to rank the components' influences, the authors apply the gradient capital allocation afterwards. Also, our article differs from papers like Breuer and Csiszár (2013) or Packham and Woebbeking (2019), who deal with adverse scenarios addressing uncertainty of the model or its calibration, while our approach provides scenarios which express the existing model. In the literature about systemic risks in financial markets, both gradient allocation as well as PCA have been employed. Chen et al. (2013) show that important systemic risk measures exhibit positive homogeneity. The authors suggest a risk attribution to individual firms which relates to the allocation in non-atomic games of Aumann and Shapley (1974) as well as to gradient capital allocation. Acharya et al. (2017) employ gradient capital allocation in order to measure how banks contribute to systemic crises and to define a tax which internalizes the related social costs. Moreover, PCA was found to be a useful measure for the interconnectedness of financial sectors (Billio et al., 2012; Rodríguez-Moreno and Peña, 2013). Similar to the extension of the gradient allocation at a company level, OCS could also be used to derive PCA-similar scenarios of systemic risk and connect the previously mentioned forms of systemic risk analysis.

The remainder of this article is structured as follows. Section 2 provides a suggestive example concerning a financial firm's RORAC outlining the limitation of the gradient capital allocation and how OCS can address it. Section 3 provides the general set-up and defines quality criteria of a scenario-based risk measurement. Section 4 defines the gradient scenario and identifies its shortcomings in terms of the defined quality criteria. PCA-scenarios are then presented and discussed. Section 5 defines OCS, presents their structural relationship with the gradient scenario and with PCA-scenarios, and shows how they make the scenario-based risk measurement suitable in terms of the quality criteria. Section 6 outlines possible applications of OCS. Section 7 concludes.

2 Motivating example: RORAC maximization

Let us consider a financial institution with three business segments. The segments can deliver random profits or losses.[5] The firm's overall potential losses are measured by the 99% Value-at-Risk of 100 monetary units. The gradient capital allocation splits the Value-at-Risk to the three segments with values $30.8 + 45.1 + 24.1 = 100$. Suppose the segments' expected profits are $1.4+2.2+1.4 = 5$. Therefore, the Return on Risk-Adjusted Capital (RORAC) of the entire firm is 5/100=5%, and based on the gradient allocation, the segments' RORACs are 1.4/30.8=4.55%, 2.2/45.1=4.87%, and 1.4/24.1=5.81%.

According to Tasche (2008, p. 428 f.), the gradient allocation is "RORAC compatible". Hence, given that the RORACs of segments 1 and 2 (segment 3) are smaller (larger) than the RORAC of the entire firm, the firm's RORAC increases when segments 1 and 2 are slightly reduced and segment 3 is slightly expanded. However, analogous to what Buch et al. (2011, p. 3006) point out for their example, it is unclear to what extent the segments should change.

We examine a portfolio change with segments 1 and 2 each reducing their businesses by 25% and segment 3 expanding by 50%. Supposing that the segments' risk contributions remain stable with the portfolio change, the gradient allocation estimates the new Value-at-Risk in terms of $0.75 \cdot 30.8 + 0.75 \cdot 45.1 + 1.5 \cdot 24.1 = 93.1$. The estimated new RORAC is therefore $(0.75 \cdot 1.4 + 0.75 \cdot 2.2 + 1.5 \cdot 1.4)/93.1 = 4.8/93.1 = 5.2\%$. However, recognizing the distribution assumptions in the example, risks of segment 3 become much more dominant in the new portfolio and the segment's contribution is severely underestimated by the given gradient allocation. In fact, the true Value-at-Risk of the new portfolio is 101.9, and the new RORAC is $4.8/101.9 = 4.7\%$, thus lower than for the initial portfolio.

We now describe the initial portfolio's risk structure using the gradient allocation and one additional orthogonal convexity scenario (OCS). In the present example, the next OCS assigns the values -19.0, -33.1 and 52.1 to the three segments. It thus points out that losses in segment 3 potentially occur at the same time as gains in segments 1 and 2 ("losses" and "gains" are interchangeable in this statement). The Value-at-Risk for the

[5] Details about the distribution assumptions are presented later in section 6.1.

new portfolio can be approximated by the root sum of squares with the two scenarios, i.e.

$$\sqrt{(0.75 \cdot 30.8 + 0.75 \cdot 45.1 + 1.5 \cdot 24.1)^2 + (0.75 \cdot (-19.0) + 0.75 \cdot (-33.1) + 1.5 \cdot 52.1)^2}$$
$$= \sqrt{93.1^2 + 39.1^2} = 100.9,$$

which is much closer to the new portfolio's true Value-at-Risk (101.9) than the estimate with only the gradient allocation (93.1). OCS thus improve describing the risk situation in the initial portfolio by incorporating important potential changes in risk concentrations.

3 Set-up

The technical basis of our considerations is a mapping from the portfolio vector $u = (u_1, ..., u_n)^{\mathrm{T}} \in \mathbb{R}^n$, with $n \in \mathbb{N}$, to a real-valued risk measurement,

$$f : U \to \mathbb{R} \tag{1}$$

with $U \subseteq \mathbb{R}^n$ being open and convex. Function $f(u)$ represents the firm's target value and will be referred to as the *original risk measurement* going forward. The vector u defines the composition of the firm's portfolio, U is the set of admissible portfolios and $u_{\text{initial}} \in U$ is the firm's initial portfolio. The technical assumption throughout our paper is

Assumption (A): *$f(u)$, as defined in (1), is positive homogeneous of degree one, i.e. for all $\lambda > 0$ we have $f(\lambda \cdot u) = \lambda \cdot f(u)$. Moreover, $f(u_{initial}) > 0$ and $f(u)$ is twice continuously differentiable at $u_{initial} \in U$.*

A classical example for specifying $f(u)$ considers an n-dimensional portfolio with vector u containing exposures to risk factors.[6] Let the random vector $\mathbf{X} = (X_1, ..., X_n)^{\mathrm{T}}$ model the losses (or gains in case of negative values) of the portfolio's n positions with finite expectations. Hence,

$$u^{\mathrm{T}}\mathbf{X} = \sum_{i=1}^{n} u_i X_i$$

[6]This specification is consistent with, for example, Gourieroux et al. (2000), Rockafellar et al. (2000), Buch and Dorfleitner (2008), Tasche (2008), and Erel et al. (2015).

is the loss (or gain) of the portfolio. Let ϱ be a law-invariant, positive homogeneous and translation-invariant risk measure.[7] The original risk measurement can then be defined as the risk measurement of unexpected portfolio losses,

$$f_{\text{stoch}} : U \to \mathbb{R}, u \mapsto \varrho\left(u^{\mathrm{T}}\mathbf{X}\right) - \mathbb{E}\left(u^{\mathrm{T}}\mathbf{X}\right) \tag{2}$$

The differentiability of $f_{\text{stoch}}(u)$ depends on the risk measure and the multivariate distribution of $\mathbf{X}$. It is discussed, for instance, in Gourieroux et al. (2000), Tasche (2008) and Hong and Liu (2009).

Assumption (A) does not require a stochastic model in terms of (2). For example, $f(u)$ can be a deterministic risk measurement in the sense of the hybrid approach of Rosenberg and Schuermann (2006).[8] Even if the risk aggregation is conducted in several steps, like in the module-submodule structure of the Solvency II standard formula, the overall capital requirement is a positive homogeneous function with respect to exposures at the submodule level.

Our target is to provide a local approximation of $f(u)$ using a measurement based on $m \in \{1, ..., n\}$ deterministic scenarios $x_1, ..., x_m \in \mathbb{R}^n$. The approximation is formalized by function $g_m(u)$:

$$g_m : \mathbb{R}^n \to \mathbb{R}, u \mapsto \sqrt{\sum_{j=1}^{m}\left(x_j^{\mathrm{T}}u\right)^2} \tag{3}$$

In terms of the stochastic approach in (2), the scenarios $x_1, ..., x_m$ can be viewed as realizations of the random vector $\mathbf{X}$.[9] For each scenario x_j, $u^{\mathrm{T}}x_j$ is the portfolio loss (or gain) conditioned on scenario x_j having been realized. In case of $m = 1$ scenario, $g_m(u)$ simplifies to $\left|x_1^{\mathrm{T}}u\right|$. For $m > 1$, the root sum of squares in (3) is analogous to risk aggregation for elliptical distributions and thus consistent with a risk measurement based on a Principal Component Analysis (PCA), as we will discuss later in section 4.2.

Going forward, we investigate how accurately $g_m(u)$ locally approximates the original risk measurement $f(u)$ at an initial portfolio u_{initial}. To this end, we will assess $g_m(u)$ based on the following "quality criteria" (QC):

[7] McNeil et al. (2015, p. 275 ff.) summarize desirable properties of risk measures.
[8] Paulusch (2017) deals with homogeneity of risk measurement in the sense of the hybrid approach.
[9] This notion of a scenario is consistent with McNeil and Smith (2012).

(QC1) ***Reflect the risk of the initial portfolio:***

For the initial portfolio $u_{initial} \in U$, we have $g_m(u_{initial}) = f(u_{initial})$.

(QC2) ***Reflect first-order sensitivities:***

Let $V_1 \subseteq \mathbb{R}^n$ be a space of possible portfolio changes. Starting from $u_{initial} \in U$, $g_m(u)$ accurately reflects the change in portfolio risk due to a marginal exposure change in the direction of $v \in V_1$, i.e.

$$\frac{\partial}{\partial h} g_m(u_{initial} + h \cdot v) \Big|_{h=0} = \frac{\partial}{\partial h} f(u_{initial} + h \cdot v) \Big|_{h=0} \quad \text{for all } v \in V_1$$

(QC3) ***Reflect second-order sensitivities:***

Let $V_2 \subseteq V_1$ be a space of possible portfolio changes. Starting from $u_{initial} \in U$, $g_m(u)$ accurately reflects second-order derivatives of portfolio risk with respect to exposure changes in the directions of $v_1, v_2 \in V_2$, i.e.

$$\begin{aligned} &\frac{\partial^2}{\partial h_1 \partial h_2} g_m(u_{initial} + h_1 \cdot v_1 + h_2 \cdot v_2) \Big|_{h_1=h_2=0} = \\ =&\frac{\partial^2}{\partial h_1 \partial h_2} f(u_{initial} + h_1 \cdot v_1 + h_2 \cdot v_2) \Big|_{h_1=h_2=0} \end{aligned}$$

for all $v_1, v_2 \in V_2$

If a scenario-based risk measurement $g_m(u)$ satisfies *(QC2)* with $V_1 = \mathbb{R}^n$, then it provides the same gradient capital allocation as the true risk measurement. According to Tasche (2008), this property is essential to signal which marginal portfolio changes enhance RORAC. Criterion *(QC3)* points out that $g_m(u)$ reflects (at least in part) the curvature of $f(u)$. It therefore aims for overcoming limitations of the gradient capital allocation, as identified for example by Buch et al. (2011).

4 Existing approaches

4.1 The gradient scenario

The gradient capital allocation principle defines an n-dimensional vector which we call the "gradient scenario" and use as a starting point of our analysis. We define

$$x^{\text{grad}} := \nabla_u f(u) \Big|_{u=u_{\text{initial}}} \tag{4}$$

Our terminology of the "gradient scenario" fits with the scenario analysis of McNeil and Smith (2012). In connection with definition (2) and the risk measure VaR, assuming a situation where VaR is coherent, the gradient scenario coincides with the so-called "Least Solvent Likely Event" (LSLE) of McNeil and Smith.[10] Irrespective of this assumption, Euler's homogeneous function theorem immediately implies that $g_1(u)$ in connection with the gradient scenario fulfills *(QC1)* and *(QC2)*.[11]

4.2 Principal component analysis (PCA)

PCA identifies important patterns of a multivariate distribution and thus allows for defining multiple scenarios. Consider the original risk measurement $f(u) = f_{\text{stoch}}(u)$ from (2). Let Σ denote the covariance matrix of $\mathbf{X}$, and let the vectors $w_i \in \mathbb{R}^n$, $i = 1, ..., n$, denote the eigenvectors of Σ. Then the random variables $w_i^{\mathrm{T}} \cdot \mathbf{X}$ and $w_j^{\mathrm{T}} \cdot \mathbf{X}$, $i \neq j$, are pairwise uncorrelated, since

$$\operatorname{cov}\left(w_i^{\mathrm{T}} \cdot \mathbf{X}, w_j^{\mathrm{T}} \cdot \mathbf{X}\right) = w_i^{\mathrm{T}} \cdot \Sigma \cdot w_j = 0 \tag{5}$$

Moreover, scenarios can be defined as

$$x_j^{\text{PCA}} := \frac{\Sigma \cdot w_j}{\sqrt{w_j^{\mathrm{T}} \Sigma w_j}} \cdot z \tag{6}$$

with $j = 1, ..., n$ and some factor $z > 0$. For two special cases, Eq. (6) allows for a proper scenario-based risk measurement, as Proposition 1 points out.

[10] The coincidence is proven by McNeil and Smith (2012) in Corollary 4.4.
[11] Cf., for example, Buch and Dorfleitner (2008).

Proposition 1. *Assume that the original risk measurement is defined by* $f(u) = f_{stoch}(u)$ *from* (2) *and that the covariance matrix* Σ *of the random vector* $\boldsymbol{X}$ *exists. For* $m \in \{1, ..., n\}$*, let* $w_1, ..., w_m \in \mathbb{R}^n$*, denote the eigenvectors of* Σ *relating to its positive eigenvalues sorted in descending order. Suppose that one of the following conditions holds:*

a. *Risk measure* ϱ *is the standard deviation. In Eq.* (6)*,* z *is set to 1.*

b. $\boldsymbol{X}$ *follows an elliptical distribution with the risk measure* ϱ *being proportional to the standard deviation by factor* $z > 0$.[12]

Define function $g_m(u)$ *according to (3) in connection with the scenarios in Eq.* (6)*. For* $u \in \text{span}\{w_1, \ldots, w_m\}$*, we have* $g_m(u) = f(u)$*. Moreover, if* $u_{initial} \in \text{span}\{w_1, \ldots, w_m\}$*,* $g_m(u)$ *satisfies (QC1), (QC2) with* $V_1 = \mathbb{R}^n$ *and (QC3) with* $V_2 = \text{span}\{w_1, \ldots, w_m\}$*.*

Hence, irrespective of the number of PCA-scenarios used, these scenarios reflect the true risk measurement in terms of the gradient allocation with respect to all risks and, to a limited extent, in terms of convexity if the conditions of Proposition 1 are fulfilled and if $u_{\text{initial}} \in \text{span}\{w_1, \ldots, w_m\}$.

The conditions in Proposition 1 are, however, quite restrictive. For downside risk measures, such as Value-at-Risk and Expected Shortfall, $\mathbf{X}$ must include neither skewed marginal distributions nor increased tail dependencies. As an example, PCA has been considered as a useful tool for measuring interest rate risks of a bond portfolio in "normal times".[13] In a low-yield environment, however, lower bounds for interest rates may become more relevant (cf. Christensen and Rudebusch, 2015), suggesting that interest rates follow a skewed distribution and implying that PCA-scenarios can not properly reflect the Value-at-Risk (cf. Schlütter, 2021).

[12]For elliptical distributions, the condition of proportionality is satisfied, e.g. for Value-at-Risk and Expected Shortfall. For example, when $\mathbf{X}$ follows a multivariate normal distribution and the risk measure is the Value-at-Risk with confidence level ζ, then the factor z is the ζ-percentile of the standard normal distribution.

[13]Cf. Frye (1997), Golub and Tilman (1997) and Hull (2018, pp. 204 ff.).

5 Orthogonal convexity scenarios (OCS)

5.1 Defining OCS

To derive a scenario-based risk measurement with useful results for non-elliptical distributions, we replace the covariance matrix with a more general measure for stochastic dependencies. Paulusch and Schlütter (2022) demonstrate that a risk measurement $f(u)$ fulfilling assumption (A) can be approximated by a deterministic function which has the structure of the hybrid approach of Rosenberg and Schuermann (2006). Specifically, the second-order Taylor polynomial of $f^2(u)$ at u_{initial} can be presented using a matrix function

$$P_{f^2}(u) = 0.5u^{\mathrm{T}}Hu \tag{7}$$

with H being the Hessian matrix of $f^2(u)$ evaluated at $u = u_{\text{initial}}$.[14] Taking the square-root on both sides of (7) provides a local approximation of $f(u)$:

$$g_{\text{Taylor}}(u) = \sqrt{P_{f^2}(u)} = \sqrt{0.5u^{\mathrm{T}}Hu} \tag{8}$$

$g_{\text{Taylor}}(u)$ reflects $f(u)$ at u_{initial} up to second-order derivatives.

Recall that the PCA builds on vectors w_i implying that the random variables $w_i^{\mathrm{T}} \cdot \mathbf{X}$ and $w_j^{\mathrm{T}} \cdot \mathbf{X}$ are pairwise uncorrelated, cf. line (5). In our proposed approach, we identify vectors $w_1, ..., w_m$ that are pairwise orthogonal in a context that allows for useful scenarios as a basis of $g_m(u)$. Mathematically, orthogonality is defined in connection with a symmetric bilinear form $\langle ., . \rangle$ and two vectors w_i, w_j are called orthogonal if $\langle w_i, w_j \rangle = 0$. Lemma 1 introduces the symmetric bilinear form that we use later on.

Lemma 1. *Let assumption (A) be fulfilled and let H denote the Hessian matrix of $f^2(u)$ evaluated at $u_{initial} \in U$. Then*

$$\begin{aligned} \langle w_i, w_j \rangle_H &:= \frac{\partial^2}{\partial h_i \partial h_j} f^2 \left(u_{initial} + h_i w_i + h_j w_j \right) \Big|_{h_i = h_j = 0} \\ &= w_i^{\mathrm{T}} H w_j \end{aligned} \tag{9}$$

defines a symmetric bilinear form on $U \times U$.

[14] Cf. Paulusch and Schlütter (2022), Theorem 1.

The basic idea behind the orthogonal convexity scenarios is to select linear independent vectors $w_1, ..., w_m \in \mathbb{R}^n$ which span a subspace $V \subseteq \mathbb{R}^n$ with $u_{\text{initial}} \in V$. The vectors $w_1, ..., w_m$ should be pairwise orthogonal in the sense of $\langle ., . \rangle_H$ and satisfy $\langle w_i, w_i \rangle_H > 0$ for all $i = 1, ..., m$. Then, any $u \in V$ can be represented as[15]

$$u = \sum_{j=1}^{m} \frac{\langle w_j, u \rangle_H}{\langle w_j, w_j \rangle_H} \cdot w_j \tag{10}$$

Let

$$\tilde{u}_j = \frac{\langle w_j, u \rangle_H}{\langle w_j, w_j \rangle_H} \cdot w_j \text{ for } j = 1, ..., m \tag{11}$$

Then we have

$$\begin{aligned} u^{\mathrm{T}} H u &= (\tilde{u}_1 + ... + \tilde{u}_m)^{\mathrm{T}} H (\tilde{u}_1 + ... + \tilde{u}_m) \\ &= \tilde{u}_1^{\mathrm{T}} H \tilde{u}_1 + ... + \tilde{u}_m^{\mathrm{T}} H \tilde{u}_m \end{aligned} \tag{12}$$

where the last equation follows from the pairwise orthogonality of the w_j (which implies pairwise orthogonality of the $\tilde{u}_j$). Lemma 2 defines vectors x_j^{OCS}, which we call *orthogonal convexity scenarios* (OCS).

Lemma 2. *Let the assumptions of Lemma 1 be fulfilled. For $m \in \{1, ..., n\}$, assume that $w_1, ..., w_m \in \mathbb{R}^n$ are pairwise orthogonal in the sense of $\langle ., . \rangle_H$ and satisfy $\langle w_i, w_i \rangle_H > 0$ for all $i = 1, ..., m$. For all $j \in \{1, ..., m\}$, define*

$$x_j^{OCS} := \frac{H w_j}{\sqrt{2 w_j^{\mathrm{T}} H w_j}} \tag{13}$$

Then

$$\left(\left(x_j^{OCS} \right)^{\mathrm{T}} u \right)^2 = 0.5 \tilde{u}_j^{\mathrm{T}} H \tilde{u}_j \tag{14}$$

with $\tilde{u}_j$ being defined as in line (11) *based on w_j and u.*

According to Eq. (13), each OCS is determined based on an underlying portfolio vector w_j. Condition $\langle w_i, w_i \rangle_H > 0$ means that $f(u)$ is locally at u_{initial} strictly convex with respect to changes in direction w_i. The assumption is satisfied, for example, if $f(u)$ is specified by Eq. (2) with a risk measure that satisfies the *convexity axiom*.

[15] Cf. for example Clay et al. (2015, p. 341), Theorem 5.

Based on Lemma 2 we can derive the OCS-based risk measurement of portfolio $u \in V$. To this end, entering Eq. (14) into Eq. (12) implies

$$g_m^2(u) = \sum_{j=1}^{m} \left(\left(x_j^{OCS} \right)^{\mathrm{T}} u \right)^2 = 0.5 \sum_{j=1}^{m} \tilde{u}_j^{\mathrm{T}} H \tilde{u}_j \overset{(12)}{=} 0.5 u^{\mathrm{T}} H u \overset{(7)}{=} P_{f^2}(u) \tag{15}$$

Taking the square-root on both sides of Eq. (15) implies that $g_m(u)$ in connection with the OCS from Eq. (13) approximates the true risk measurement $f(u)$ in the sense of a second-order Taylor approximation at $u = u_{\text{initial}}$. Theorem 1 outlines this result.

Theorem 1. *Let the assumptions of Lemma 2 be fulfilled and assume that* $u_{initial} \in \text{span}\{w_1, ..., w_m\}$. *Then* $g_m(u)$ *as defined in line* (3) *in connection with the scenarios* x_j^{OCS} *defined in Eq.* (13)*, for* $j = 1, ..., m$*, fulfills (QC1), (QC2) with* $V_1 = \mathbb{R}^n$ *and (QC3) with* $V_2 = \text{span}\{w_1, \ldots, w_m\}$. *For* $u \in \text{span}\{w_1, \ldots, w_m\}$*, we have* $g_m(u) = g_{Taylor}(u)$.

The statements of Theorem 1 are analogous to those of Proposition 1. Hence, OCS allow a generalization of the PCA-based risk measurement with respect to skewed distributions and increased tail dependencies.

The condition $u_{\text{initial}} \in \text{span}\{w_1, ..., w_m\}$ can be ensured by setting $w_1 = u_{\text{initial}}$. Corollary 1 shows that the corresponding first OCS then coincides with the gradient scenario defined in Eq. (4).

Corollary 1. *Let the assumptions of Lemma 1 be fulfilled and* $w_1 = u_{initial}$. *Then we have*

$$x_1^{OCS} = x^{grad}$$

with x_1^{OCS} *being defined as in Eq.* (13) *and* x^{grad} *as in Eq.* (4).

Therefore, OCS can consistently extend the concept of the gradient scenario as introduced in Section 3.1: in addition to the gradient scenario, portfolio risk is communicated with the scenarios $x_2^{\text{OCS}}, ..., x_m^{\text{OCS}}$. Based on these scenarios, $g_m(u)$ not only accurately reflects marginal portfolio changes (as it does based on the single gradient scenario), but also reflects how diversification effects alter when the portfolio is changed in directions within the subspace V_2.

The selection of the OCS, i.e. the selection of the vectors $w_1, ..., w_m$, determines the space V_2 for which the scenario-based risk measurement $g_m(u)$ meets the curvature of $f(u)$ in the sense of *(QC3)*, cf. Theorem 1. The selection should therefore be made against the background of practical considerations, such that V_2 contains conceivable portfolio changes in light of restrictions of the firm's overall strategy, regulation, etc.

Section 5.2 provides guidance on the selection of OCS in the general case. Afterwards, section 5.3 explains the selection for an analysis in which the addition of a particular portfolio segment is of interest.

5.2 Selecting OCS

This section proposes an iterative approach to select the most meaningful OCS. In this regard, we aim to minimize the approximation error and note that the approximation error for any portfolio $u \in U$ can be decomposed into two parts:

$$f(u) - g_m(u) = \underbrace{f(u) - g_{\text{Taylor}}(u)}_{\text{Error part 1}} + \underbrace{g_{\text{Taylor}}(u) - g_m(u)}_{\text{Error part 2}} \tag{16}$$

Only the error part 2 depends on the employed scenarios. For $m = n$ OCS being used, error part 2 is zero for all portfolios u. To select a further scenario, we therefore focus on the error part 2.

Suppose that m vectors $w_1, ..., w_m$ have been selected in line with the assumptions of Lemma 2 and with $u_{\text{initial}} \in \text{span}\{w_1, ..., w_m\}$. Based on these vectors, scenarios have been determined with Eq. (13). With Eq. (10), we can write any $u \in U$ as

$$u = \underbrace{\sum_{j=1}^{m} \frac{\langle w_j, u \rangle_H}{\langle w_j, w_j \rangle_H} \cdot w_j}_{=:\tilde{u}} + u_{\text{remainder}} \tag{17}$$

Given that $\langle u_{\text{remainder}}, w_i \rangle_H = 0$ for all $i = 1, ..., m$, we focus on the subset of vectors that are orthogonal to $w_1, ..., w_m$,

$$U_\perp = \Big\{ u \in \mathbb{R}^n \text{ such that } \langle u, w_i \rangle_H = 0 \text{ for all } i = 1, ..., m \Big\}, \tag{18}$$

Starting from an arbitrary portfolio $\tilde{u} \in \text{span}\{w_1, ..., w_m\}$, we identify vector $w_{m+1} \in U_\perp$ with the largest error type 2, i.e.

$$w_{m+1} = \text{argmax}\Big\{g_{\text{Taylor}}(\tilde{u} + w) - g_m(\tilde{u} + w) \text{ with } w \in U_\perp \text{ and } \|w\|_2 = 1\Big\} \tag{19}$$

Appendix B shows that the searched vector w_{m+1} does not depend on $\tilde{u} \in \text{span}\{w_1, ..., w_m\}$, and can be rewritten as

$$\text{argmax}\Big\{g_{\text{Taylor}}(w) \text{ with } w \in U_\perp \text{ and } \|w\|_2 = 1\Big\} \tag{20}$$

Moreover, the Appendix shows that w_{m+1} can be identified as the solution of an eigenvalue problem provided that H is positive semidefinite. Adding a further scenario based on w_{m+1} in connection with Eq. (13) ensures that the error type 2 is eliminated in the identified direction, i.e. $g_{m+1}(\tilde{u} + w_{m+1}) = g_{\text{Taylor}}(\tilde{u} + w_{m+1})$.

5.3 OCS on the surface of an ellipsoid

As a starting point for risk visualizations, Corollary 2 shows that the scenarios defined by Eq. (13) are on the surface of an ellipsoid. For $n = 2$ or $n = 3$, the ellipsoid can be added into a scatter plot of realizations of the random vector X.

Corollary 2. *Let the assumptions of Lemma 2 be fulfilled and assume that H is invertible. Then, all scenarios x_j^{OCS} as defined by Eq.* (13) *are on the surface of the ellipsoid*

$$\{v \in \mathbb{R}^n \mid v^{\mathrm{T}} H^{-1} v \leq 0.5\} \tag{21}$$

As an example for a situation which allows a two-dimensional visualization, we analyze the situation of adding a particular asset to a preexisting portfolio. Formally, we consider $n = 2$ risks with X_1 reflecting the risks of the preexisting portfolio, X_2 the risks of the asset of interest and $u_{\text{initial}} = (1, 0)^{\mathrm{T}}$. For this "contribution analysis", Corollary 3 derives two OCS which inform about the first and second-order sensitivity of the portfolio's aggregate risk with respect to adding X_2.

Corollary 3. *Let the assumptions of Lemma 2 be fulfilled with $n = 2$ and $u_{initial} = (1, 0)^{\mathrm{T}}$, and let h_{ij} denote the entries of H. We set $w_1 = u_{initial}$, $w_2 = (-h_{12}/h_{11}, 1)^{\mathrm{T}}$ and*

determine x_1^{OCS} *and* x_2^{OCS} *by Eq.* (13)*. Let* x_{ij}^{OCS} *denote entry* j *of vector* x_i^{OCS}*. We have* $x_{21}^{OCS} = 0$ *and the function value, gradient and Hessian matrix are given by*

$$\begin{aligned} f(u_{\text{initial}}) &= x_{11}^{\text{OCS}} \\ \nabla_u f(u_{\text{initial}}) &= x_1^{\text{OCS}} \\ H_f(u_{\text{initial}}) &= \begin{pmatrix} 0 & 0 \\ 0 & \frac{\left(x_{22}^{\text{OCS}}\right)^2}{x_{11}^{\text{OCS}}} \end{pmatrix} \end{aligned}$$

Based on the two OCS defined in Corollary 3, the ellipsoid from line (21) can be added into a two-dimensional scatter plot of realizations of X_1 and X_2. We will call the ellipsoid in this context the "contribution ellipsoid". It allows us to link the marginal impact and the convexity of adding X_2 for the aggregate portfolio risk with the scatter plot.

5.4 Example: Multivariate elliptical distribution

For the case of X following a multivariate elliptical distribution, some of our results about OCS can be linked to well-known concepts.

Proposition 2. *Let the assumptions of Proposition 1 be fulfilled. We have*

a. $H = 2z^2\Sigma$

b. For given $w_1, ..., w_m$*, we have* $x_j^{OCS} = x_j^{PCA}$ *as defined in Eq.* (13) *and* (6)*.*

c. Vectors $w_1, ..., w_m$ *being the eigenvectors of* Σ *corresponding to positive eigenvalues in descending order satisfy the selection approach in section 5.2.*

d. For $z = 1$*, the ellipsoid defined in line* (21) *coincides with the ellipsoid of concentration introduced by Darmois (1945), which is defined as*[16]

$$\{v \in \mathbb{R}^n : v^{\mathrm{T}}\Sigma^{-1}v \leq 1\} \tag{22}$$

e. Let $w_1 = u_{initial}$*. Then each entry* j *of* x_1^{OCS} *satisfies*

$$x_{1j}^{OCS} = \beta_j \cdot f(u_{initial})$$

[16]This definition is used by Nordström (1991, p. 397).

with

$$\beta_j = \frac{cov\left(X_j, \boldsymbol{X}^{\mathrm{T}} \cdot u_{initial}\right)}{var\left(\boldsymbol{X}^{\mathrm{T}} \cdot u_{initial}\right)}$$

Assertion b. means that OCS scenarios coincide with PCA-scenarios when the conditions of Proposition 2 are fulfilled and the vectors $w_1, ...w_m$ are the eigenvectors of Σ. According to assertion d., the ellipsoid in line (21) is a stretched version from the ellipsoid of Darmois (1945) if $z > 1$. It is also a shifted and stretched or compressed version of the ellipsoid of concentration proposed by Cramér (1946).[17]

Assertion e. points out that the first OCS (i.e. the gradient capital allocation) relates to the Capital Asset Pricing Model (CAPM) of Sharpe (1964), Lintner (1965) and Mossin (1966). For multivariate normal distributions, this relation was already shown by Panjer (2002), who refers to the β_j as "internal betas". Starting from this notion, convexity of portfolio risk is driven by the residuals of an (internal) CAPM-like regression of the profits of each portfolio segment on the total portfolio's profits. Higher OCS point out which group of segments exhibit volatile and highly correlated residuals.

6 Applications

6.1 Analyzing a portfolio of business segments

We consider a financial institution with three segments as in section 2. The random vector $X = (X_1, X_2, X_3)^{\mathrm{T}}$ models the segments' losses (positive realizations) or gains (negative realizations). The vector $u \in \mathbb{R}^3$ reflects the sizes of segments, with the initial portfolio being characterized by $u_{\text{initial}} = (1, 1, 1)^{\mathrm{T}}$. The distributions of X_2 and X_3 are right-skewed (lognormal and Gamma), while X_1 is normally distributed. The stochastic dependencies of X_1 and X_2 are modeled by a Gumbel copula with a parameter $\Theta = 2$ which models increased tail dependencies. The dependency of $X_1 + X_2$ and X_3 is modeled by a Gaussian copula with correlation parameter $\rho = 0$. The true risk measurement $f(u)$ is defined by Eq. (2) in connection with the 99% Value-at-Risk, and we have $f(u_{\text{initial}}) = 100$. Figure 1 summarizes the distribution assumptions and presents the

[17] The statement follows immediately with the definition in Nordström (1991, p. 397).

univariate risks and the gradient scenario. The gradient scenario points out that segment 2 is currently the most dominant risk in the portfolio.

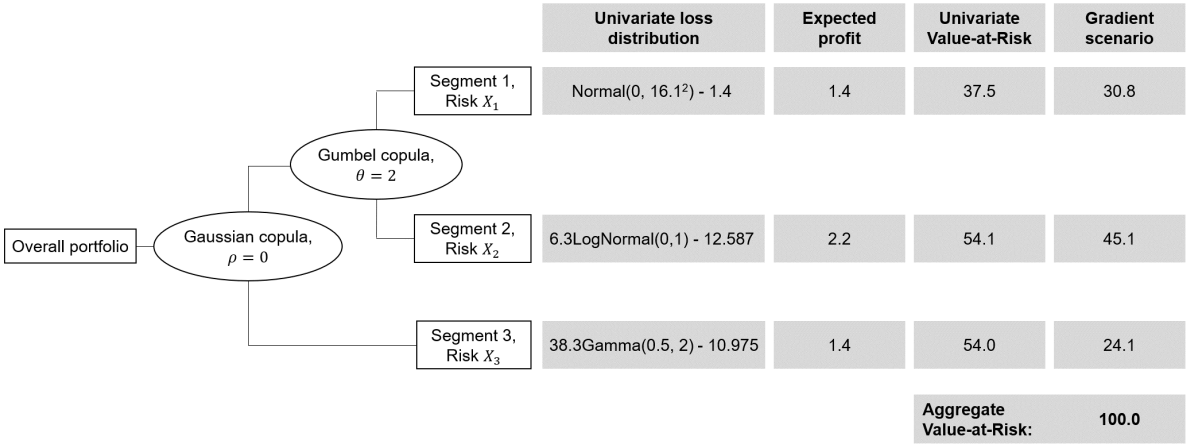

	Univariate loss distribution	Expected profit	Univariate Value-at-Risk	Gradient scenario
Segment 1, Risk X_1	Normal(0, 16.1^2) - 1.4	1.4	37.5	30.8
Segment 2, Risk X_2	6.3LogNormal(0,1) - 12.587	2.2	54.1	45.1
Segment 3, Risk X_3	38.3Gamma(0.5, 2) - 10.975	1.4	54.0	24.1
			Aggregate Value-at-Risk:	**100.0**

Figure 1: Distribution assumptions of the numerical example with three risks, X_1, X_2 and X_3. Column "Expected profit" shows the expectation of each random variable multiplied with -1 (since positive realizations reflect losses and negative reflect gains); column "Univariate Value-at-Risk" depicts $VaR_{0.99}(X_i) - E(X_i)$; the gradient scenario in the last column is determined as $\nabla_u f(u) \mid_{u=u_{initial}}$.

Table 1 presents the OCS and PCA-scenarios.[18] The first OCS is selected as the gradient scenario and thus replicates the last column of Figure 1. The last row of Table 1 the relative error between $g_m(u)$ and $g_{\text{Taylor}}(u)$,

$$\text{Max. error part 2} = \frac{\left| g_{\text{Taylor}}(u_{m+1}) - g_m(u_{m+1}) \right|}{g_{\text{Taylor}}(u_{m+1})}, \tag{23}$$

with portfolio u_{m+1} being selected as in Eq. (20).

For a risk measurement based solely on the gradient scenario, we identify portfolio $u_2 = (0.71, 0.49, 1.81)^{\text{T}}$ which is falsely assessed with $x^{\text{grad}} \cdot u_2 = 87.2$. In fact, diversification effects decrease in u_2, and the true risk hence amounts to $f(u_2) = 107.0$. The Taylor approximation is $g_{\text{Taylor}}(u_2) = 108.7$, and we thus calculate

$$\text{Max. error part 2} = \frac{|108.7 - 87.2|}{108.7} = 19.6\% \tag{24}$$

[18] To select the OCS, we have set $w_1 = u_{\text{initial}}$. Weightvectors w_2 and w_3 have been selected, successively minimizing the error between the stochastic risk measurement $f(u)$ and the approximation $g_m(u)$ as outlined in Appendix B. PCA-scenarios have been determined according to Eq. (6). The calculations are based on Monte Carlo simulations of $(X_1, X_2, X_3)^{\text{T}}$ with 1,000,000 simulation paths.

The second OCS is determined by incorporating $w_2 = u_2$ into Eq. (13). In this OCS, a loss in segment 3 is accompanied by gains in the first two segments. Hence, it states that portfolio risk increases when segment 3 is expanded and the first two segments are reduced. Such a portfolio restructuring would reduce favorable diversification effects between $X_1 + X_2$ on the one hand and X_3 on the other hand. The loss potential of segment 3, modeled by the right-skewed Gamma distribution, would therefore become a more relevant driver of the portfolio's tail risk.

In the third OCS, a loss in segment 1 is accompanied by a gain in segment 2 (and a small gain in segment 3). This scenario points out that an expansion of segment 1 with a reduction of segment 2 (or the other way around) would reduce favorable diversification effects between these two segments.

The left part of Table 2 shows how the OCS-based risk measurement evaluates non-marginal segment expansions. For segment 2, an expansion can be well estimated by the gradient scenario (with an error of -2.0%), given that segment 2 is already the dominant risk driver and expanding this segment does not materially impact diversification effects. Using a second OCS makes a small contribution and allows a reduction of the error to 0.5%. Segment 3 is not the dominant risk driver in the initial portfolio, and hence its expansion has a more convex influence on the aggregate risk. Therefore, the gradient scenario causes a relatively large error of -8.6%, and the second OCS helps to reduce the error to -0.9%.

The PCA-scenarios in the right part of Table 1—from a qualitative point of view—describe the risk situation similarly to the OCS. In the first and second PCA-scenario, losses occur in the first two segments simultaneously or in the third segment respectively. The third PCA-scenario is similar to the third OCS. Using all three PCA-scenarios, the scenario-based risk measurement of the initial portfolio, i.e. $g_3^{\mathrm{PCA}}(u_{\mathrm{initial}})$, is very close to 100 and hence almost correct. However, the PCA-scenarios do not point out that segment 2 is currently the dominant risk driver. Therefore, $g_3(u)$ substantially understates the sensitivity of the aggregate portfolio risk with respect to the size of segment 2:

$$\frac{\partial}{\partial u_2} g_3^{\mathrm{PCA}}\left(u_{\mathrm{initial}}\right) = 30.2 < 45.1 = \frac{\partial}{\partial u_2} f\left(u_{\mathrm{initial}}\right) \tag{25}$$

	OCS			PCA		
Segment i	x_{1i} (Gradient)	x_{2i} (2nd OCS)	x_{3i} (3rd OCS)	x_{1i}	x_{2i}	x_{3i}
1	30.8	-18.9	12.7	47.5	-3.8	9.9
2	45.1	-33.2	-10.6	35.6	-5.2	-13.1
3	24.1	52.1	-2.1	6.9	52.8	-0.6
Max. error part 2	19.6%	1.6%	0.0%	42.0%	18.9%	17.6%

Table 1: OCS and PCA-scenarios for the example from section 6.1. The last row shows the maximal error part 2 as defined in Eq. (23).

u_{new}	$f(u_{\text{new}})$	$g_m^{\text{OCS}}(u_{\text{new}})$			$g_m^{\text{PCA}}(u_{\text{new}})$		
		$m=1$	$m=2$	$m=3$	$m=1$	$m=2$	$m=3$
$(1,2,1)^{\text{T}}$	148.1	145.1	148.9	149.3	125.7	131.5	132.6
		(−2.0%)	(0.5%)	(0.8%)	(−15.1%)	(−11.2%)	(−10.5%)
$(1,1,2)^{\text{T}}$	135.8	124.1	134.6	134.6	97.0	136.9	136.9
		(−8.6%)	(−0.9%)	(−0.9%)	(−28.6%)	(0.8%)	(0.8%)

Table 2: We consider two potential new portfolios, $u_{\text{new}} = (1,2,1)^{\text{T}}$ and $u_{\text{new}} = (1,1,2)^{\text{T}}$, i.e. expansions of segment 2 or segment 3. Column $f(u_{\text{new}})$ depicts the true risk measurements, i.e. the 99% Value-at-Risk of unexpected losses for the new portfolio. Columns under $g_m^{\text{OCS}}(u_{\text{new}})$ provide the risk measurement based on $m = 1$, 2 or 3 OCS. Columns under $g_m^{\text{PCA}}(u_{\text{new}})$ provide the risk measurement based on PCA-scenarios. The lower lines provide relative errors between scenario-based and true risk measurement (i.e. errors part 1 and 2 from Eq. (16) in total). Errors beyond 5% (10%) are highlighted in (dark) grey.

Therefore, the PCA-based risk measurement leads to substantial misevaluations for portfolios in an environment of u_{initial}, as shown in the last row of Table 1. Specifically, the right part of Table 2 points out that a non-marginal expansion of segment 2 is measured based on PCA-scenarios with an error of −10.5% even if all three PCA scenarios are used.

6.2 Risk visualization

Figure 2 presents the ellipsoid as defined in (21) in a scatter plot of 50,000 realizations of the random vector $(X_1, X_2, X_3)^{\text{T}}$. Realizations with an aggregate loss above the 99% Value-at-Risk, i.e. $x_1 + x_2 + x_3 > f(u_{\text{initial}}) = 100$, are colored in red; the others are colored in gray. The black plane satisfies $x_1 + x_2 + x_3 = 100$ and thus separates the red and gray realizations. We call this plane the VaR-plane, since it marks realizations with an aggregate loss that equals the portfolio's Value-at-Risk. The blue line reflects the gradient scenario, the two green lines reflect the other two OCS.

The plot on the left-hand side of Figure 2 shows that the ellipse is wide in the direction of the second OCS, pointing out that the risks of segment 3 are currently well diversified with those of segments 1 and 2 for realizations that are close to the VaR-plane, and that risks of segment 3 could become more dominant if this segment were to be expanded. The plot on the right-hand side shows that the ellipse is narrow from the perspective of the x_1-x_2 plane: given that risks of segments 1 and 2 are highly correlated along the VaR-plane, an exchange of these risks would hardly impact the aggregate Value-at-Risk.

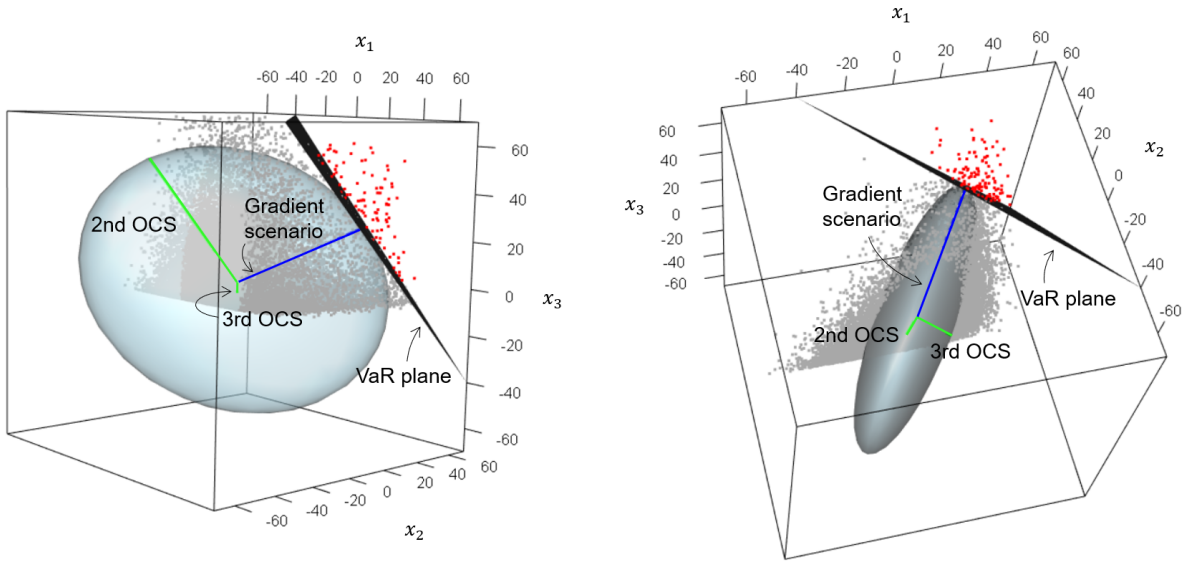

Figure 2: The 3d plots show 50,000 realizations of $(X_1, X_2, X_3)^{\mathrm{T}}$ and the ellipsoid from (21) from two perspectives. The blue line depicts the gradient scenario; the green lines depict the second and third OCS.

We next continue the example with a contribution analysis, as described in section 5.3. The upper part of Figure 3 investigates an expansion of segment 2. In light of section 5.3, we consider $X_1 + X_2 + X_3$ as the risks of the pre-existing portfolio and X_2 as risks which are to be added. The left-hand side of Figure 3 presents the contribution ellipsoid in a scatter plot of realizations of portfolio returns, $X_1 + X_2 + X_3$, vs. realizations of X_2, X_3. On the right-hand side, the blue curve depicts function

$$\tilde{f}(h) = \varrho(X_1 + X_2 + X_3 + h \cdot X_i)$$

for $i = 2, 3$; the red line depicts a first-order approximation of it based on the gradient scenario, i.e. $\tilde{g}_1(h)$ as in Eq. (3). The y-coordinate of the respective gradient scenario $\tilde{x}_1^{OCS}$ on the left-hand side coincides with the increase of the red line from $h = 0$ to 1 as

stated in Corollary 3. The green curve on the right-hand side depicts $\tilde{g}_2(h)$ and hence additionally includes x_2^{OCS} in the approximation of $\tilde{f}(h)$. The y-coordinate of the second OCS, $\tilde{x}_2^{OCS}$, directly relates to the convexity of $\tilde{f}(h)$, as also stated in Corollary 3.

Comparing contribution ellipsoids in the upper and lower parts of Figure 3 exhibits two differences of the segments. Firstly, due to the larger y-coordinate of $\tilde{x}_1^{\text{OCS}}$, the ellipsoid of segment 2 is directed upwards more strongly than for segment 3, pointing out that X_2 is connected more strongly to tail risks of the portfolio than X_3. Secondly, because of the larger y-coordinate of $\tilde{x}_1^{\text{OCS}}$, the contribution ellipsoid of segment 3 is wider than the one for segment 2. Consequently, a non-marginal extension of segment 3 can make X_3 a dominant risk in the portfolio, and $\tilde{f}(h)$ is hence more curved for segment 3 than for segment 2.

6.3 Risk limiting

In their "Principles for An Effective Risk Appetite Framework", the Financial Stability Board (2013, p. 6. f.) requires financial institutions to install risk limits in order to allocate their aggregate risk appetite to lower levels such as business segments or risk categories. In this sense, the gradient capital allocation could be a starting point for risk limits, as it points out how much a marginal expansion of segments affects the company's risk. If several segments change their volumes adversely, the composition of diversification effects changes, and hence the segments' contributions to the company's overall risk alter. Therefore, the initially defined risk limits may become ineffective. Buch et al. (2011, p. 3005) propose limits that build on the gradient capital allocation per business segment. To ensure that the aggregate limit is not breached, the authors include a parameter Λ, which is an upper bound for the largest eigenvalue of the Hessian matrix of $f(u)$ on the set of portfolios U. A drawback of their approach is that Λ does not recognize that convexity may vary across segments, i.e. that volume changes in some segments may change the risk profile of the portfolio more immediately than others. We now outline an approach that overcomes this drawback.

Suppose the firm from section 6.1 holds enough equity capital to increase the aggregate Value-at-Risk from 100 to 120. OCS allow for a natural starting point to define risk limits in two stages: a first-order limit is based on the gradient scenario controlling the

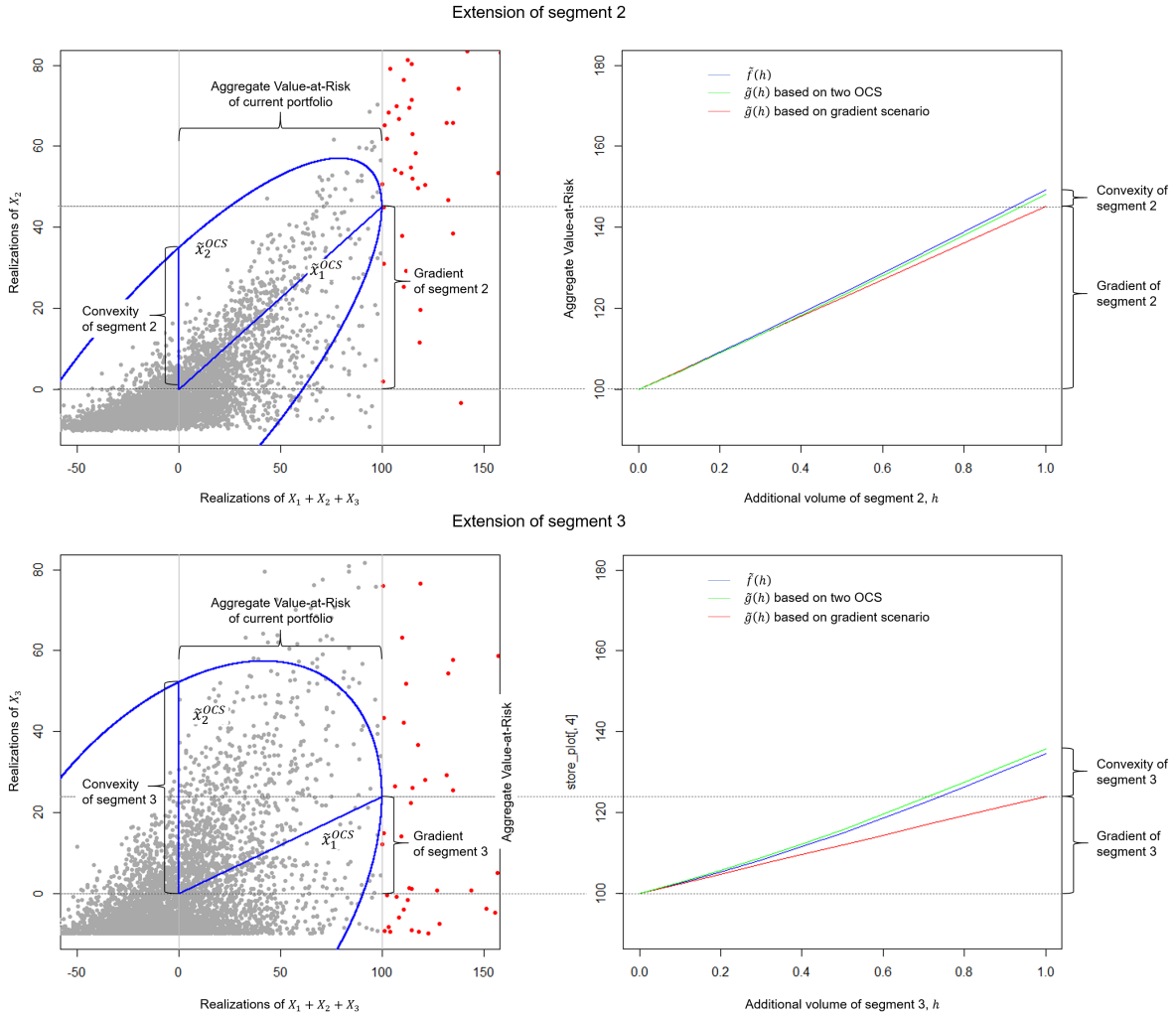

Figure 3: Left hand-side: scatter plot of X_2 (bottom part) and X_3 (lower part) vs. $X_1 + X_2 + X_3$ with contribution ellipsoids and OCS. Right part: Aggregate Value-at-Risk according to true risk measurement (blue curve), gradient scenario (red line) and first two OCS (green curve).

aggregate risk conditioned on the portfolio composition not having changed too much. In addition, second-order limits based on additional OCS control the stability of the portfolio composition.

The left side of Figure 4 depicts combinations of u_1 and u_2 with $u_3 = 1$ being fixed; the right side of the Figure depicts combinations of u_1 and u_3 with $u_2 = 1$ being fixed. The combinations below the green curve are admissible if risk limits are implemented based on the true risk measurement, i.e.

$$f(u) \leq 120$$

Using the OCS in Table 1, we allocate limits as

$$\left|\left(x_1^{OCS}\right)^{\mathrm{T}} u\right| \leq \sqrt{120^2 - 2 \cdot 15^2} = 118.11 \tag{26}$$

$$\left|\left(x_2^{OCS}\right)^{\mathrm{T}} u\right| \leq 15 \tag{27}$$

$$\left|\left(x_3^{OCS}\right)^{\mathrm{T}} u\right| \leq 15 \tag{28}$$

ensuring that

$$g_m(u) \leq 120$$

The left-hand sides of Ineq. (26) - (28) are linear in u_i and depicted in Figure 4 by the red line (gradient scenario), blue lines (second OCS) and dashed blue lines (third OCS). The gray colored area marks portfolios that meet all limits in Ineq. (26) - (28). In the u_1u_2-plane on the left-hand side Figure 4, the area of admissible portfolios is wider than in the u_1u_3-plane on the right-hand side: a substitution of the risks of segment 1 with those of segment 2 hardly impacts the risk profile given that they are both strongly connected with each other through the Gumbel copula. In contrast, if risks of segment 1 are substituted with those of segment 3, the risk profile changes more immediately, since risks of segment 3—which are currently well diversified—become more dominant for the risk profile.

A practical implementation of the proposed limits in the given example could be that segments are allowed to increase their business by up to 20% (first-order limits) and a central department regularly supervises the adherence to second-order limits. If a second-order limit is breached, first-order limits have to be adjusted. Limits in the sense of Ineq. (26) - (28) should be conservative and account for a potential remainder of $f(u) - g_m(u)$, i.e. the right-hand sides of these inequalities should add up to a total limit of $120 - \max_{u \in U} |f(u) - g_m(u)|$.[19] In the given example, $g_m(u)$ slightly overestimates $f(u)$, and the remainder hence does not appear in the limits.

[19] Starting points for assessing the remainder are provided by Paulusch and Schlütter (2022) Proposition 1 and Appendix I.

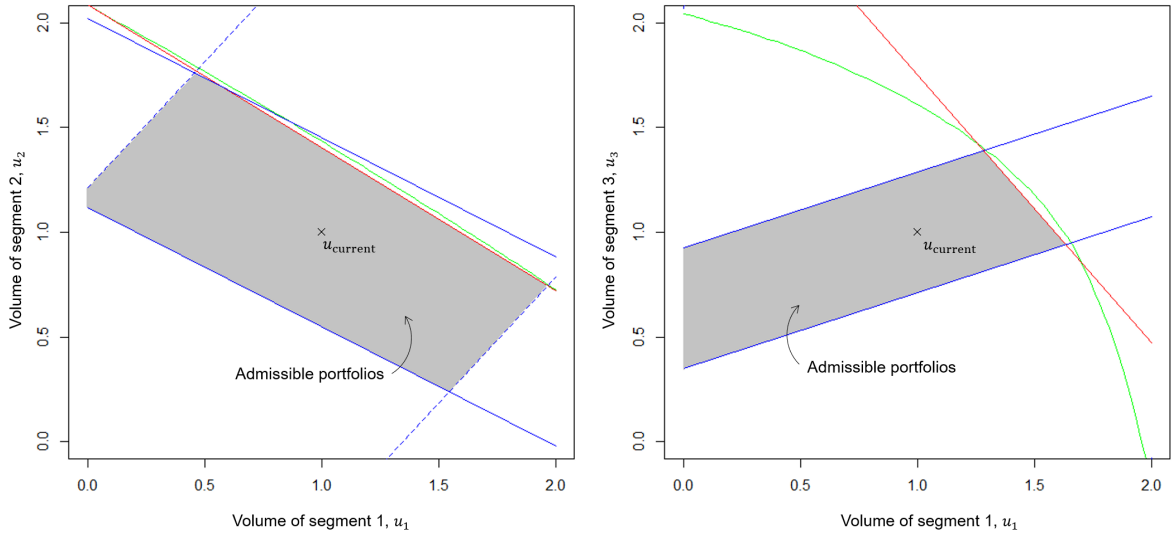

Figure 4: Risk limits. The green curves reflect u_1u_2-combinations (left side, $u_3 = 1$ is fixed), and u_1u_3-combinations (right side, $u_2 = 1$ is fixed), such that $f(u_1, u_2, u_3) = 120$. The red lines reflect combinations satisfying the gradient scenario limit in Ineq. (26) with equality. The blue lines (dashed blue lines) reflect combinations satisfying the further OCS limits in Ineq. (27) (Ineq. (28)) with equality. The gray colored area marks portfolios meeting all limits in Ineq. (26) - (28).

7 Conclusion

This paper proposes a new methodology for translating portfolio risk into multivariate scenarios of portfolio segments' profits and losses. Our proposed orthogonal convexity scenarios (OCS) extend the gradient capital allocation principle in the sense that they inform about second-order sensitivities of portfolio risk with respect to the volumes of portfolio segments. Specifically, OCS demonstrate which combinations of expansions or reductions of portfolio segments can cause a substantial amplification of risk concentrations. OCS can also be viewed as a generalization of Principal Component Analysis, providing a second-order local approximation of portfolio risk without the need for assuming an elliptical distribution. We demonstrate applications of OCS in terms of risk communication, visualization and risk limiting.

Our central Assumption (A) requires the risk measurement to be homogeneous in the vector of decision variables. Limitations to this assumption may arise if idiosyncratic risks within a segment change with the segment's volume, which may be particularly relevant for insurance risks. To overcome this limitation, the literature offers starting

points based on Lévy processes, allowing for a homogeneous approximation (Mildenhall, 2017) and a meaningful gradient allocation (Boonen et al., 2017).

Throughout this article, we assume that the risk model, i.e. the original risk measurement $f(u)$, is well established and allows for calculating first and second-order derivatives. The estimation of first- and/or second-order derivatives based on sample data or a Monte Carlo simulation is addressed in many articles, for example, in Gourieroux et al. (2000), Hong and Liu (2009), Gómez et al. (2022), Gribkova et al. (2022), Paulusch and Schlütter (2022). It seems promising that OCS can favor the estimation of second-order derivatives. For this purpose, one could set up an iterative process that uses OCS to identify particularly relevant directional derivatives to which the estimation could pay special attention. We leave this however beyond the scope of this paper and for future research.

Appendix

A Proofs

A.1 Proof of Proposition 1

Note that the standard deviation of $u^{\mathrm{T}}\mathbf{X}$ is $\sqrt{u^{\mathrm{T}}\Sigma u}$. Therefore, in both cases a. and b., the original risk measurement can be written as

$$f(u) = z \cdot \sqrt{u^{\mathrm{T}}\Sigma u} \tag{29}$$

with a constant $z > 0$. For all $u \in \operatorname{span}\{w_1, ..., w_m\}$, there are constants $\lambda_1, ..., \lambda_m \in \mathbb{R}$ such that

$$u = \sum_{i=1}^{m} \lambda_i w_i \tag{30}$$

and we have

$$\begin{aligned}
g_m^2(u) = \sum_{j=1}^{m} \left(\left(x_j^{PCA}\right)^{\mathrm{T}} u \right)^2 &\overset{\text{Eq. (6)}}{=} z^2 \cdot \sum_{j=1}^{m} \left(\frac{w_j^{\mathrm{T}} \cdot \Sigma}{\sqrt{w_j^{\mathrm{T}}\Sigma w_j}} \cdot u \right)^2 \\
&\overset{\text{Eq. (30)}}{=} z^2 \cdot \sum_{j=1}^{m} \left(\frac{w_j^{\mathrm{T}} \cdot \Sigma}{\sqrt{w_j^{\mathrm{T}}\Sigma w_j}} \cdot \sum_{i=1}^{m} \lambda_i w_i \right)^2 = z^2 \cdot \sum_{i,j=1}^{m} \lambda_i^2 \cdot \left(\frac{w_j^{\mathrm{T}} \cdot \Sigma \cdot w_i}{\sqrt{w_j^{\mathrm{T}}\Sigma w_j}} \right)^2 \\
&\overset{\text{Eq. (5)}}{=} z^2 \cdot \sum_{i=1}^{m} \lambda_i^2 \cdot \left(\frac{w_i^{\mathrm{T}} \cdot \Sigma \cdot w_i}{\sqrt{w_i^{\mathrm{T}}\Sigma w_i}} \right)^2 = z^2 \cdot \sum_{i=1}^{m} \lambda_i^2 \cdot w_i^{\mathrm{T}} \cdot \Sigma \cdot w_i \\
&\overset{\text{Eq. (30)}}{=} z^2 \cdot u^{\mathrm{T}} \cdot \Sigma \cdot u \overset{\text{Eq. (29)}}{=} f^2(u)
\end{aligned}$$

By definition in lines (3) and (29), $g_m(u) \geq 0$ and $f(u) \geq 0$. Therefore, $g_m^2(u) = f^2(u)$ implies $g_m(u) = f(u)$. For $u_{\text{initial}} \in \operatorname{span}\{w_1, ..., w_m\}$, the statements about $(QC1)$ and $(QC3)$ thus follow immediately.

A.2 Proof of Lemma 1

With assumption (A), the second equation of (9) holds because the differential operator is linear. $\langle ., . \rangle_H$ defines a symmetric bilinear form, since we have for all $w_1, w_2, w_3 \in U$ and all $\lambda \in \mathbb{R}$: (i) $\langle w_1, w_2 \rangle_H = w_1^{\mathrm{T}} H w_2 = w_2^{\mathrm{T}} H w_1 = \langle w_2, w_1 \rangle_H$ due to the symmetry of

H; (ii) $\langle w_1 + w_2, w_3\rangle_H = (w_1 + w_2)^{\mathrm{T}} H w_3 = w_1^{\mathrm{T}} H w_3 + w_2^{\mathrm{T}} H w_3 = \langle w_1, w_3\rangle_H + \langle w_2, w_3\rangle_H$; (iii) $\langle \lambda \cdot w_1, w_2\rangle_H = (\lambda \cdot w_1)^{\mathrm{T}} H w_2 = \lambda \cdot w_1^{\mathrm{T}} H w_2 = \lambda \cdot \langle w_1, w_2\rangle_H$.

A.3 Proof of Lemma 2

We have

$$\begin{aligned}\left(\left(x_j^{\mathrm{OCS}}\right)^{\mathrm{T}} u\right)^2 &\overset{\text{Eq. (13)}}{=} \left(\left(\frac{Hw_j}{\sqrt{2w_j^{\mathrm{T}} Hw_j}}\right)^{\mathrm{T}} u\right)^2 = \frac{1}{2w_j^{\mathrm{T}} Hw_j} \cdot (w_j^{\mathrm{T}} Hu)^2 = \frac{\left(\langle w_j, u\rangle_H\right)^2}{2\langle w_j, w_j\rangle_H} \\ &= \frac{\left(\langle w_j, u\rangle_H\right)^2}{2\left(\langle w_j, w_j\rangle_H\right)^2} \cdot w_j^{\mathrm{T}} Hw_j = 0.5 \cdot \left(\frac{\langle w_j, u\rangle_H}{\langle w_j, w_j\rangle_H} \cdot w_j\right)^{\mathrm{T}} H \left(\frac{\langle w_j, u\rangle_H}{\langle w_j, w_j\rangle_H} \cdot w_j\right) \\ &\overset{\text{Eq. (11)}}{=} 0.5 \tilde{u}_j^{\mathrm{T}} H \tilde{u}_j\end{aligned}$$

A.4 Proof of Theorem 1

By definition in lines (3) and (8), $g_m(u) \geq 0$ and $g_{\mathrm{Taylor}}(u) \geq 0$ for all $u \in U$. Hence, Eq. (15) implies $g_m(u) = g_{\mathrm{Taylor}}(u)$ for all $u \in \mathrm{span}\{w_1, ..., w_m\}$. This implies $(QC1)$. According to Theorem 1 from Paulusch and Schlütter (2022), $g_{\mathrm{Taylor}}(u)$ satisfies $(QC2)$ and $(QC3)$ with $V_1 = V_2 = \mathbb{R}^n$. Since $g_m(u) = g_{\mathrm{Taylor}}(u)$ for $u \in \mathrm{span}\{w_1, ..., w_m\}$, we can conclude that $(QC3)$ holds with $V_2 = \mathrm{span}\{w_1, ..., w_m\}$. Focusing on $(QC2)$, we calculate with the definition of OCS in Eq. (13) in connection with Eq. (3)

$$g_m^2(u) = \sum_{i=1}^{m} \left(\left(x_i^{OCS}\right)^{\mathrm{T}} u\right)^2 = \sum_{i=1}^{m} \left(\frac{w_i^{\mathrm{T}} Hu}{\sqrt{2w_i^{\mathrm{T}} Hw_i}}\right)^2$$

The gradient of $g_m^2(u)$ evaluated at u_{initial} is obtained as

$$\nabla_u g_m^2(u_{\mathrm{initial}}) = 2 \cdot \sum_{i=1}^{m} \frac{w_i^{\mathrm{T}} Hu_{\mathrm{initial}}}{2w_i^{\mathrm{T}} Hw_i} \cdot w_i^{\mathrm{T}} H$$

Given that $u_{\mathrm{initial}} \in \mathrm{span}\{w_1, \ldots, w_m\}$, we can write analogously to Eq. (10)

$$u_{\mathrm{initial}} = \sum_{j=1}^{m} \frac{\langle w_j, u_{\mathrm{initial}}\rangle_H}{\langle w_j, w_j\rangle_H} \cdot w_j \tag{31}$$

Noting that $w_i H w_j = 0$ for all $i \neq j$, we have

$$\begin{aligned} \nabla_u g_m^2 \left(u_{\text{initial}}\right) &= \sum_{i,j=1}^{m} \frac{\langle w_j, u_{\text{initial}} \rangle_H}{\langle w_j, w_j \rangle_H} \frac{w_i^{\mathrm{T}} H w_j}{w_i^{\mathrm{T}} H w_i} \cdot w_i^{\mathrm{T}} H = \sum_{i=1}^{m} \frac{\langle w_i, u_{\text{initial}} \rangle_H}{\langle w_i, w_i \rangle_H} \cdot w_i^{\mathrm{T}} H \\ &= u_{\text{initial}}^{\mathrm{T}} H \overset{\text{Eq. (7)}}{=} \nabla_u P_{f^2} \left(u_{\text{initial}}\right) \end{aligned} \tag{32}$$

According to Assumption (A), $f(u) > 0$ in an environment of u_{initial}. Therefore, line (32) implies

$$\nabla_u g_m \left(u_{\text{initial}}\right) = \nabla_u g_{\text{Taylor}} \left(u_{\text{initial}}\right) = \nabla_u f \left(u_{\text{initial}}\right), \tag{33}$$

where the last equality follows from Theorem 1 of Paulusch and Schlütter (2022).

A.5 Proof of Corollary 1

We have

$$\begin{aligned} x^{\text{grad}} &= \nabla_u f(u_{\text{initial}}) \overset{\text{Eq. (33)}}{=} \nabla_u g_m \left(u_{\text{initial}}\right) \overset{\text{Eq. (8)}}{=} \nabla_u \sqrt{0.5 u^{\mathrm{T}} H u} \Big|_{u=u_{\text{initial}}} \\ &= \frac{H u_{\text{initial}}}{\sqrt{2 u_{\text{initial}}^{\mathrm{T}} H u_{\text{initial}}}} \overset{\text{Eq. (13)}}{=} x_1^{\text{OCS}} \end{aligned}$$

where the last equation uses $w_1 = u_{\text{initial}}$.

A.6 Proof of Corollary 2

For all $j = 1, \ldots, m$, we have

$$\begin{aligned} \left(x_j^{OCS}\right)^{\mathrm{T}} H^{-1} x_j^{OCS} &\overset{\text{Eq. (13)}}{=} \frac{1}{2 w_j^{\mathrm{T}} H w_j} \cdot w_j^{\mathrm{T}} H^{\mathrm{T}} H^{-1} H w_j \\ &\overset{\text{H is symmetric}}{=} \frac{1}{2 w_j^{\mathrm{T}} H w_j} \cdot w_j^{\mathrm{T}} H w_j = 0.5 \end{aligned}$$

A.7 Proof of Corollary 3

w_1 and w_2, as defined, are orthogonal in the sense of $\langle ., . \rangle_H$, since

$$w_1^{\mathrm{T}} H w_2 = (1, 0) \cdot \begin{pmatrix} 0 \\ -h_{12}^2 / h_{11} + h_{22} \end{pmatrix} = 0$$

Inserting w_2 into Eq. (13) implies

$$x_2^{OCS} = \frac{1}{\sqrt{2(h_{22} - h_{12}^2/h_{11})}} \begin{pmatrix} 0 \\ h_{22} - h_{12}^2/h_{11} \end{pmatrix} = \frac{1}{\sqrt{2}} \begin{pmatrix} 0 \\ \sqrt{h_{22} - h_{12}^2/h_{11}} \end{pmatrix} \tag{34}$$

Corollary 1 implies $\nabla_u f(u_{\text{initial}}) = x_1^{\text{OCS}}$. Together with Euler's homogeneous function theorem, we have

$$f(u_{\text{initial}}) = (\nabla_u f(u_{\text{initial}}))^{\text{T}} \cdot u_{\text{initial}} = \left(x_1^{\text{OCS}}\right)^{\text{T}} \cdot u_{\text{initial}} = x_{11}^{\text{OCS}} \tag{35}$$

Let $H_g(u)$ and $H_{g^2}(u)$ denote the Hessian matrices of functions $g(u)$ and $g^2(u)$ evaluated at u. The chain rule and product rule for multivariate functions imply

$$\begin{aligned}
H_{g^2}(u_{\text{initial}}) &= \nabla_u \left[2g(u) \left(\nabla_u g(u)\right)^{\text{T}}\right] \Big|_{u=u_{\text{initial}}} \\
&= 2\nabla_u g(u) \left(\nabla_u g(u)\right)^{\text{T}} + 2g(u) H_g(u) \Big|_{u=u_{\text{initial}}} \\
\Leftrightarrow H_g(u_{\text{initial}}) &= \frac{1}{g(u)} \left(0.5 H_{g^2}(u) - \nabla_u g(u) \left(\nabla_u g(u)\right)^{\text{T}}\right) \Big|_{u=u_{\text{initial}}} \\
\overset{\text{Theorem 1}}{\Leftrightarrow} H_f(u_{\text{initial}}) &= \frac{1}{f(u)} \left(0.5 H - \nabla_u f(u) \left(\nabla_u f(u)\right)^{\text{T}}\right) \Big|_{u=u_{\text{initial}}} \\
&\overset{\text{Eq. (35)}}{=} \frac{1}{x_{11}^{\text{OCS}}} \left(0.5 H - x_1^{\text{OCS}} \left(x_1^{\text{OCS}}\right)^{\text{T}}\right)
\end{aligned} \tag{36}$$

Inserting $w_1 = (1, 0)^{\text{T}}$ into Eq. (35) provides

$$\begin{aligned}
x_1^{\text{OCS}} \left(x_1^{\text{OCS}}\right)^{\text{T}} &= \frac{1}{2 w_1^{\text{T}} H w_1} H w_1 \left(H w_1\right)^{\text{T}} = \frac{1}{2 h_{11}} \begin{pmatrix} h_{11} \\ h_{12} \end{pmatrix} (h_{11}, h_{12}) \\
&= \frac{1}{2} \begin{pmatrix} h_{11} & h_{12} \\ h_{12} & h_{12}^2/h_{11} \end{pmatrix}
\end{aligned} \tag{37}$$

Inserting line (37) into (36) implies that entry (2,2) of $H_f(u_{\text{initial}})$ is

$$\frac{1}{2 x_{11}^{\text{OCS}}} \left(h_{22} - h_{12}^2/h_{11}\right) \overset{\text{Eq. (34)}}{=} \frac{\left(x_{21}^{\text{OCS}}\right)^2}{x_{11}^{\text{OCS}}}$$

and that all other entries of $H_f(u_{\text{initial}})$ are zero.

A.8 Proof of Proposition 2

a. Line (29) implies $f^2(u) = z^2 \cdot u^{\mathrm{T}}\Sigma u$ and $H = \nabla_u \left(z^2 \cdot 2\Sigma u\right)|_{u=u_{\text{initial}}} = 2z^2\Sigma$.

b. Starting from the definition in line (13) and using assertion a., we have

$$x_j^{OCS} = \frac{Hw_j}{\sqrt{2w_j^{\mathrm{T}}Hw_j}} = \frac{2z^2\Sigma w_j}{\sqrt{2w_j^{\mathrm{T}}2z^2\Sigma w_j}} = \frac{\Sigma w_j}{\sqrt{w_j^{\mathrm{T}}\Sigma w_j}} \cdot z = x_j^{\mathrm{PCA}}$$

c. To identify w_1, we can neglect condition $\langle u, w_i\rangle_H = 0$ in $U_\perp$ from Eq. (18), since there are no formerly selected w_i. Then, the eigenvector of Σ relating to its largest eigenvalue solves Eq. (20) noting that $g^2_{\text{Taylor}}(u) = z^2u^{\mathrm{T}}\Sigma u$. Due to $H = 2z^2\Sigma$, the eigenvalues of Σ are a multiple of those of H, and the two matrices' eigenvectors coincide. With vectors $w_1, ..., w_m$ being identified as eigenvectors corresponding to the m largest eigenvalues, the columns of matrix M in Appendix B can be set to the eigenvectors relating to the other positive eigenvalues of Σ. Therefore, $\Lambda = M^{\mathrm{T}}HM$ includes the remaining eigenvalues of H. Since $M^{\mathrm{T}}M$ is the identity matrix of dimension $\tilde{n} - m$, the smallest eigenvalue of $\Lambda^{-0.5}M^{\mathrm{T}}M\Lambda^{-0.5}$ is the inverse of the largest eigenvalue of H, say $\lambda_{\max}^{-1}$. w_{m+1} from Eq. (40) is the corresponding eigenvector of Σ, since

$$w_{m+1}^{\mathrm{T}}\Sigma w_{m+1} = \frac{w_{m+1}^{\mathrm{T}}Hw_{m+1}}{2z^2} = \frac{s^{\mathrm{T}}\Lambda^{-0.5}M^{\mathrm{T}}HM\Lambda^{-0.5}s}{2z^2s^{\mathrm{T}}\Lambda^{-0.5}M^{\mathrm{T}}M\Lambda^{-0.5}s} = \frac{s^{\mathrm{T}}s}{2z^2\lambda_{\max}^{-1}} = \frac{\lambda_{\max}}{2z^2}$$

d. With $z = 1$, the conditions in lines (21) and (22) are equivalent, since $v^{\mathrm{T}}H^{-1}v \leq 0.5 \Leftrightarrow v^{\mathrm{T}}(2\Sigma)^{-1}v \leq 0.5 \Leftrightarrow v^{\mathrm{T}}\Sigma^{-1}v \leq 1$.

e. With assertion b. and $w_1 = u_{\text{initial}}$, noting that Corollary 1 implies $x_1^{\text{OCS}} = x_1^{\text{grad}}$ and using Eq. (29), we have

$$\frac{x_{1j}^{\text{OCS}}}{f(u_{\text{initial}})} = \frac{\left(\frac{\Sigma w_1}{\sqrt{w_1^{\mathrm{T}}\Sigma w_1}} \cdot z\right)_j}{z \cdot \sqrt{u_{\text{initial}}^{\mathrm{T}}\Sigma u_{\text{initial}}}} = \frac{\Sigma_{j.} \cdot u_{\text{initial}}}{u_{\text{initial}}^{\mathrm{T}}\Sigma u_{\text{initial}}} = \frac{\text{cov}\left(X_j, \mathbf{X}^{\mathrm{T}} \cdot u_{\text{initial}}\right)}{\text{var}\left(\mathbf{X}^{\mathrm{T}} \cdot u_{\text{initial}}\right)} = \beta_j$$

B Lagrange procedure for OCS selection

We start with the Lagrangian for identifying w_{m+1}, i.e.

$$L_1(w, \gamma_0, \gamma_1, ..., \gamma_m) = g_{\text{Taylor}}(\tilde{u} + w) - g_m(\tilde{u} + w) + \gamma_0 \cdot \left(w^{\text{T}} w - 1\right) + \sum_{i=1}^{m} \gamma_i \cdot w_i^{\text{T}} H w$$

In this Lagrangian, we can omit the term $g_m(\tilde{u} + w)$, since it vanishes in the first-order condition: for any $w \in U_\perp$, we have $g_m(\tilde{u} + w) = g_m(\tilde{u})$, and hence $\nabla_w g_m(\tilde{u} + w) = 0$. Since the target function $g_{\text{Taylor}}(\tilde{u} + w)$ is non-negative, we can replace it with its square and rewrite

$$\begin{aligned} g^2_{\text{Taylor}}(\tilde{u} + w) &= 0.5 \cdot (\tilde{u} + w)^{\text{T}} H (\tilde{u} + w) = 0.5 \cdot \left(\tilde{u}^{\text{T}} H \tilde{u} + 2\tilde{u}^{\text{T}} H w + w^{\text{T}} H w\right) \\ &= 0.5 \tilde{u}^{\text{T}} H \tilde{u} + 0.5 w^{\text{T}} H w \end{aligned}$$

Omitting the constant term and the factor 0.5, the target function becomes $w^{\text{T}} H w$.

Let $\tilde{n} \leq n$ denote the rank of H. We assume that $m < \tilde{n}$, since Theorem 1 otherwise implies that there is no remaining error part 2. Define a matrix $M \in \mathbb{R}^{n \times (\tilde{n}-m)}$ with $\text{rank}(HM) = \tilde{n} - m$, $Mv \in U_\perp$ for all $v \in \mathbb{R}^{\tilde{n}-m}$ and the columns of M being orthogonal in the sense of $\langle ., . \rangle_H$. To ensure that $w \in U_\perp$, we set $w = Mv$ and identify v maximizing $g^2_{\text{Taylor}}(Mv)$ using the simpler Lagrangian

$$L_2(v, \gamma) = v^{\text{T}} M^{\text{T}} H M v + \gamma \left(v^{\text{T}} M^{\text{T}} M v - 1\right) \tag{38}$$

We define $\Lambda = M^{\text{T}} H M$, which by construction is a diagonal matrix with all diagonal elements being positive, since $\text{rank}(HM) = \tilde{n} - m$ and H is positive semidefinite. Let $\lambda_1, ..., \lambda_{\tilde{n}-m}$ denote the diagonal elements of Λ and let the matrix $\Lambda^{-0.5}$ be a diagonal matrix with diagonal entries $\lambda_1^{-0.5}, ..., \lambda_{\tilde{n}-m}^{-0.5}$. We substitute $v = \Lambda^{-0.5} s$ and rewrite the Lagrangian in line (38) as

$$\begin{aligned} L_2(s, \gamma) &= s^{\text{T}} \Lambda^{-0.5} \Lambda \Lambda^{-0.5} s + \gamma s^{\text{T}} \Lambda^{-0.5} M^{\text{T}} M \Lambda^{-0.5} s \\ &= s^{\text{T}} s + \gamma s^{\text{T}} \Lambda^{-0.5} M^{\text{T}} M \Lambda^{-0.5} s \end{aligned}$$

The first-order condition of maximizing $L_2(s, \gamma)$ includes

$$\nabla_s L_2(s, \gamma) = 2s + 2\gamma\Lambda^{-0.5} M^{\mathrm{T}} M \Lambda^{-0.5} s = 0 \tag{39}$$

which is satisfied if s is an eigenvector of $\Lambda^{-0.5} M^{\mathrm{T}} M \Lambda^{-0.5}$. We select s relating to the smallest eigenvalue of $\Lambda^{-0.5} M^{\mathrm{T}} M \Lambda^{-0.5}$. Finally, we determine portfolio w_{m+1} with the largest approximation error and satisfying $\|w_{m+1}\|_2 = 1$ as

$$w_{m+1} = \frac{1}{\sqrt{s^{\mathrm{T}} \Lambda^{-0.5} M^{\mathrm{T}} M \Lambda^{-0.5} s}} \cdot M \Lambda^{-0.5} s \tag{40}$$

Scenario w_{m+2} can immediately be identified by inserting the eigenvector relating to the second smallest eigenvalue into line (40) and so on.

References

Acharya, V.V., Pedersen, L.H., Philippon, T., Richardson, M., 2017. Measuring systemic risk. The Review of Financial Studies 30, 2–47.

Aumann, R.J., Shapley, L.S., 1974. Values of non-atomic games. Princeton University Press.

Aven, T., 2016. Risk assessment and risk management: Review of recent advances on their foundation. European Journal of Operational Research 253, 1–13.

Bauer, D., Zanjani, G., 2016. The marginal cost of risk, risk measures, and capital allocation. Management Science 62, 1431–1457.

Billio, M., Getmansky, M., Lo, A.W., Pelizzon, L., 2012. Econometric measures of connectedness and systemic risk in the finance and insurance sectors. Journal of Financial Economics 104, 535–559.

Boonen, T.J., Tsanakas, A., Wüthrich, M.V., 2017. Capital allocation for portfolios with non-linear risk aggregation. Insurance: Mathematics and Economics 72, 95–106.

Borgonovo, E., Plischke, E., 2016. Sensitivity analysis: A review of recent advances. European Journal of Operational Research 248, 869–887.

Breuer, T., Csiszár, I., 2013. Systematic stress tests with entropic plausibility constraints. Journal of Banking & Finance 37, 1552–1559.

Buch, A., Dorfleitner, G., 2008. Coherent risk measures, coherent capital allocations and the gradient allocation principle. Insurance: Mathematics and Economics 42, 235–242.

Buch, A., Dorfleitner, G., Wimmer, M., 2011. Risk capital allocation for RORAC optimization. Journal of Banking & Finance 35, 3001–3009.

Chen, C., Iyengar, G., Moallemi, C.C., 2013. An axiomatic approach to systemic risk. Management Science 59, 1373–1388.

Christensen, J.H., Rudebusch, G.D., 2015. Estimating shadow-rate term structure models with near-zero yields. Journal of Financial Econometrics 13, 226–259.

Clay, D., Lay, S.R., McDonald, J.J., 2015. Linear Algebra and Its Applications, 5th Edition. Pearson.

Cramér, H., 1946. A contribution to the theory of statistical estimation. Scandinavian Actuarial Journal 1946, 85–94.

Darmois, G., 1945. Sur les limites de la dispersion de certaines estimations. Revue de l'Institut International de Statistique , 9–15.

Eling, M., Schmeiser, H., 2010. Insurance and the credit crisis: Impact and ten consequences for risk management and supervision. The Geneva Papers on Risk and Insurance–Issues and Practice 35, 9–34.

Erel, I., Myers, S.C., Read Jr, J.A., 2015. A theory of risk capital. Journal of Financial Economics 118, 620–635.

Financial Stability Board, 2013. Principles for an effective risk appetite framework. Consultative Document, July .

Frye, J., 1997. Principals of risk: Finding var through factor-based interest rate scenarios, in: VAR: Understanding and Applying Value at Risk. Risk Publications, London, pp. 275–288.

Golub, B.W., Tilman, L.M., 1997. Measuring yield curve risk using principal components analysis, value at risk, and key rate durations. Journal of Portfolio Management 23, 72.

Gómez, F., Tang, Q., Tong, Z., 2022. The gradient allocation principle based on the higher moment risk measure. Journal of Banking & Finance 143, 106544.

Gourieroux, C., Laurent, J.P., Scaillet, O., 2000. Sensitivity analysis of values at risk. Journal of Empirical Finance 7, 225–245.

Gribkova, N., Su, J., Zitikis, R., 2022. Inference for the tail conditional allocation: large sample properties, insurance risk assessment, and compound sums of concomitants. Insurance: Mathematics and Economics 107, 199–222.

Gründl, H., Schmeiser, H., 2007. Capital allocation for insurance companies—what good is it? Journal of Risk and Insurance 74, 301–317.

Hong, L.J., Liu, G., 2009. Simulating sensitivities of conditional value at risk. Management Science 55, 281–293.

Hull, J.C., 2018. Risk Management and Financial Institutions. Wiley Finance Series. 5th Edition.

Jorion, P., 2006. Value at risk: The new benchmark for managing financial risk. New York: McGrow–Hill .

Kang, W.Y., Poshakwale, S., 2019. A new approach to optimal capital allocation for rorac maximization in banks. Journal of Banking & Finance 106, 153–165.

Landsman, Z., Makov, U., 2011. Translation-invariant and positive-homogeneous risk measures and optimal portfolio management. The European Journal of Finance 17, 307–320.

Lintner, J., 1965. Security prices, risk, and maximal gains from diversification. The Journal of Finance 20, 587–615.

McNeil, A.J., Frey, R., Embrechts, P., 2015. Quantitative Risk Management: Concepts, Techniques and Tools - Revised Edition. Princeton Series in Finance.

McNeil, A.J., Smith, A.D., 2012. Multivariate stress scenarios and solvency. Insurance: Mathematics and Economics 50, 299–308.

Mildenhall, S.J., 2017. Actuarial geometry. Risks 5, 31.

Mossin, J., 1966. Equilibrium in a capital asset market. Econometrica: Journal of the Econometric Society , 768–783.

Nordström, K., 1991. The concentration ellipsoid of a random vector revisited. Econometric Theory 7, 397–403.

Packham, N., Woebbeking, C., 2019. A factor-model approach for correlation scenarios and correlation stress testing. Journal of Banking & Finance 101, 92–103.

Panjer, H.H., 2002. Measurement of risk, solvency requirements and allocation of capital within financial conglomerates. Institute of Insurance and Pension Research, University of Waterloo, Research Report , 01–15.

Paulusch, J., 2017. The Solvency II standard formula, linear geometry, and diversification. Journal of Risk and Financial Management 10, 11.

Paulusch, J., Schlütter, S., 2022. Sensitivity-implied tail-correlation matrices. Journal of Banking & Finance 134, 106333.

Rockafellar, R.T., Uryasev, S., et al., 2000. Optimization of conditional value-at-risk. Journal of Risk 2, 21–42.

Rodríguez-Moreno, M., Peña, J.I., 2013. Systemic risk measures: The simpler the better? Journal of Banking & Finance 37, 1817–1831.

Rosenberg, J.V., Schuermann, T., 2006. A general approach to integrated risk management with skewed, fat-tailed risks. Journal of Financial Economics 79, 569–614.

Schilling, K., Bauer, D., Christiansen, M.C., Kling, A., 2020. Decomposing dynamic risks into risk components. Management Science 66, 5738–5756.

Schlütter, S., 2021. Scenario-based measurement of interest rate risks. The Journal of Risk Finance 22 No. 1, 56–77.

Sharpe, W.F., 1964. Capital asset prices: A theory of market equilibrium under conditions of risk. The Journal of Finance 19, 425–442.

Stulz, R.M., 2008. Risk management failures: What are they and when do they happen? Journal of Applied Corporate Finance 20, 39–48.

Tasche, D., 2008. Capital allocation to business units and sub-portfolios: The Euler principle, in: Resti, A. (Ed.), Pillar II in the New Basel Accord: The Challenge of Economic Capital. Risk Books, London, pp. 423–453.

Wilson, T.C., 2015. Value and Capital Management: A Handbook for the Finance and Risk Functions of Financial Institutions, 1st Edition. Wiley.